A Canonical Transformation Theory from Extended Normal Ordering

Takeshi Yanai* and Garnet Kin-Lic Chan
Department of Chemistry and Chemical Biology
Cornell University, Ithaca, NY 14853-1301
(Dated: November 1, 2018)

The Canonical Transformation theory of Yanai and Chan [J. Chem. Phys. **124**, 194106 (2006)] provides a rigorously size-extensive description of dynamical correlation in multireference problems. Here we describe a new formulation of the theory based on the extended normal ordering procedure of Mukherjee and Kutzelnigg [J. Chem. Phys. **107**, 432 (1997)]. On studies of the water, nitrogen, and iron-oxide potential energy curves, the Linearised Canonical Transformation Singles and Doubles theory is competitive in accuracy with some of the best multireference methods, such as the Multireference Averaged Coupled Pair Functional, while computational timings (in the case of the iron-oxide molecule) are two-three orders of magnitude faster and comparable to those of Complete Active Space Second-Order Perturbation Theory. The results presented here are greatly improved both in accuracy and in cost over our earlier study as the result of a new numerical algorithm for solving the amplitude equations.

I. INTRODUCTION

While nondynamic correlation between electrons establishes the qualitative features of chemical bonding, it is the accurate description of dynamic correlation, associated with the short-range cusp behaviour of the wavefunction, which is necessary to obtain quantitative agreement with experiment. Starting from a suitable reference function, the exponential ansatz provides an accurate and economical description of dynamic correlation. For example, in systems that are qualitatively described by a single determinant reference, Coupled Cluster (CC) theory paired with a large basis set yields predictions with chemical accuracy [1, 2, 3]. However, for the many chemical problems which require a multireference characterisation, a practical theory for dynamic correlation with the desirable qualities of the exponential ansatz - size-extensivity, chemical-accuracy, and moderate computational cost - has yet to be widely established.

In an earlier article [4] we presented a Canonical Transformation (CT) theory which is based on an exponential ansatz, is rigorously size-extensive, and which may easily be combined with any multireference starting wavefunction. In the form implemented in that work the computational cost is $O(a^2 e^4)$, where a is the number of active orbitals and e is the number of external orbitals. In calculations of bond-breaking potential energy curves, the Linearised Canonical Transformation Doubles (L-CTD) theory performed significantly better than multireference perturbation theory, and obtained the accuracy of Coupled Cluster Single Doubles (CCSD) at the equilibrium geometry across the *entire* potential energy curve. Our work was directly motivated by the Canonical Diagonalisation theory of White [5] although there are earlier re-

lated contributions as we describe below.

The purpose of the current work is to improve on our initial contribution in several areas. A central feature of the Canonical Transformation theory is the use of an *operator decomposition*, both to close the infinite expansions associated with an exponential ansatz and to reduce the complexity of the energy and amplitude equations that arise when working with a complicated reference function. In our earlier work, we introduced a cumulant-type operator decomposition by analogy to the cumulant decomposition of density matrices found in reduced density matrix theories [6, 7, 8, 9, 10, 11]. However, this choice of operator decomposition is not unique and here we explore an alternative operator decomposition, with some formal advantages, that is based on the concept of *extended normal ordering* as introduced by Mukherjee and Kutzelnigg [12, 13, 14]. Indeed, examination of the articles by these authors shows that they anticipated the utility of their results in multireference correlation theories, and in this context our current theory is in part a realisation along such directions.

A second focus of this work is to investigate in detail the behaviour of the Canonical Transformation theory in a variety of chemical problems. For example we study, with a range of basis sets, the bond-breaking potential energy curves of water, nitrogen, and iron-oxide and compare our results against state-of-the-art multi-reference configuration interaction and perturbation theories. In addition, we examine numerically the size-extensivity and density-scaling properties of the Canonical Transformation energies. The results in the present study are much improved over our earlier work, in large part because of improvements we have made to our numerical algorithms, and we describe in detail the numerical aspects of efficiently implementing and converging the CT equations.

---

*Present address: Department of Theoretical and Computational Molecular Science, Institute for Molecular Science, Okazaki, Aichi 444-8585, Japan. Electronic mail: yanait@ims.ac.jp

II.   CANONICAL TRANSFORMATION THEORY

A.   Recapitulation

In multireference problems we divide the orbitals into *active orbitals*, which describe the nondynamic correlation and *external orbitals* which describe the dynamic correlation. The external orbitals may further be divided into core and virtual orbitals; core orbitals are those which remain doubly occupied in all the reference configurations.

We will assume that a reference wavefunction Ψ_0 is available that describes the nondynamic correlation in the problem. This may be obtained, for example, from a Complete Active Space Self-Consistent Field (CASSCF) calculation that exactly correlates electrons within the active orbitals [15, 16]. Alternatively, and especially for larger active spaces, a Density Matrix Renormalization Group wavefunction may be used [17, 18]. We then incorporate the remaining dynamic correlation on top of the reference wavefunction Ψ_0 via an exponential operator that generates excitations between the active and external spaces yielding

$$\Psi = e^A \Psi_0 \tag{1}$$

We will be concerned with a *unitary* formulation, where $A^\dagger = -A$. The excitations are understood to be both of external and semi-internal form

$$A = A_i^a(a_i^a - a_a^i) + A_{ij}^{ab}(a_{ij}^{ab} - a_{ab}^{ij}) + A_{ij}^{ak}(a_{ij}^{ak} - a_{ak}^{ij}) + \ldots \tag{2}$$

where $ijk\ldots$ denote active indices, $abc\ldots$, external indices, $a_i^a = a_a^\dagger a_i$, $a_{ij}^{ab} = a_a^\dagger a_b^\dagger a_j a_i$, and the summation convention is assumed. For example, the first two terms are the usual external single and double excitations, while the third term (with three active indices) is a semi-internal single excitation, which captures the coupling between singles relaxation in the active space and singles excitation to the external space.

In a related picture, we can also view e^A as generating an effective *canonically transformed* Hamiltonian $\bar{H}$ that acts only in the active space, but which has dynamic correlation folded in from the external space, where

$$\bar{H} = e^{-A} H e^A \tag{3}$$
$$\bar{H}\Psi = E\Psi \tag{4}$$

The exponential ansatz combined with a multireference wavefunction Ψ_0 as shown in eqn. (1) has a long history and we necessarily can only give an incomplete account here. Such an ansatz is used in some forms of multi-reference coupled cluster theory (MRCC) as discussed in the review by Paldus and Li [19]. In particular, an early example of a complete theoretical scheme for a related multi-reference coupled cluster method was given by Mukherjee in Ref. [12]. While CC theory is usually formulated in terms of similarity rather than canonical (i.e. unitary) transforms, unitary exponentials have

previously been explored in a multi-reference setting by Freed et al [20], Kirtman et al [21], and Simons et al [22]. We mention also the single-reference unitary coupled cluster work by Kutzelnigg [23, 24], Bartlett et al [25, 26, 27], and Pal [28, 29]. The general concept of effective Hamiltonians and canonical transformations is of course very old, dating back to van Vleck [30]. We note in particular some modern theories that emphasize an effective Hamiltonian language similar to our own such as the Effective Valence Hamiltonian theory of Freed [20] and the Generalized van Vleck theory of Kirtman [21]. As recognised by Freed, the folding in of dynamic correlation into the active-space effective Hamiltonian is a form of renormalisation transformation. This picture was pursued by White in his theory of Canonical Diagonalisation [5], and as described previously, this is the primary precursor to our work.

In the exponential ansatz of single-reference coupled cluster theory, the commutativity of the excitation operators in the single-reference form of A, i.e. $A = A_i^a a_i^a + A_{ij}^{ab} a_{ij}^{ab}$, allows the Baker-Campbell-Hausdorff expansion of $\bar{H}$ to terminate at low-order for low-particle rank in A. The difficulty in working with the multireference exponential ansatz arises from the non-commuting excitations in the multi-reference form of A in eqn. (2), which leads to a non-terminating expansion for the effective Hamiltonian $\bar{H}$. (In fact this difficulty already arises if we use a *unitary* e^A with the single-reference form of A).

In our earlier Canonical Transformation (CT) theory we introduced a new route to a tractable and computationally efficient formulation for the multireference ansatz (1). Starting from the Baker-Campbell-Hausdorff expansion of the exact effective Hamiltonian,

$$\bar{H} = H + [H, A] + \frac{1}{2}[[H, A], A] + \ldots \tag{5}$$

we replace each commutator by an approximate *decomposed* commutator, to yield an approximate effective Hamiltonian

$$\bar{H}_{1,2,\ldots} = H + [H, A]_{1,2,\ldots} + \frac{1}{2}[[H, A]_{1,2,\ldots}, A]]_{1,2,\ldots} + \ldots \tag{6}$$

Each subscript denotes a decomposition, and the numbers $1, 2 \ldots$ denote the particle ranks of the operators that remain after the decomposition. Note that if *all* particle ranks were included in the decomposition (i.e. the subscripts ranged from $1, 2, \ldots n$, where n is the number of particles), then eqns. (5) and (6) would be identical. If in addition to including all particle ranks in eqn. (6) A contained up to n-body excitations, then the CT ansatz (1) would be exact in the sense of full configuration interaction, and indeed eqn. (4) would hold exactly. The two relevant approximations thus arise from restricting the excitations in A (wavefunction ansatz) as well as the form of the operator decomposition (operator ansatz) [55].

As an example, let us consider the linearised CT single and doubles theory (L-CTSD) introduced in our earlier

work. Here A is restricted to contain only one- and two-particle excitations as in eqn. (2), and we restrict all decomposed commutators to contain at most one and two-body operators (i.e. subscripts $1, 2$). Since $[H, A]$ generates a three-body operator, this requires some decomposition of a three-body operator into lower body operators. We proposed an explicit decomposition into one- and two-body operators based on an analogy to the cumulant decomposition of density matrices,

$$a_{stu}^{pqr} \Rightarrow 9(\gamma_s^p \wedge a_{tu}^{qr}) - 12(\gamma_s^p \wedge \gamma_t^q \wedge a_u^r) \qquad (7)$$

where in the above $\wedge$ denotes an antisymmetrisation over all upper and lower indices with an associated factor of $1/(p!)^2$, i.e. $1/36$ in the above case, where p is the particle rank of the original operator. Here we will present the explicit steps leading to the above decomposition. Our notation follows closely that of Kutzelnigg and Mukherjee [31]. Recall that the cumulant decomposition provides a way to rewrite reduced density matrices γ in terms of products of cumulants λ, via

$$\gamma_s^p = \langle a_s^p \rangle = \lambda_s^p \qquad (8)$$
$$\gamma_{st}^{pq} = \langle a_{st}^{pq} \rangle = \lambda_{st}^{pq} + \gamma_s^p \gamma_t^q - \gamma_t^p \gamma_s^q \qquad (9)$$
$$\begin{aligned} \gamma_{stu}^{pqr} = \langle a_{stu}^{pqr} \rangle = {} & \lambda_{stu}^{pqr} + \gamma_s^p \lambda_{tu}^{qr} - \gamma_t^p \lambda_{su}^{qr} + \gamma_u^p \lambda_{st}^{qr} \\ & -\gamma_s^q \lambda_{tu}^{pr} + \gamma_t^q \lambda_{su}^{pr} - \gamma_u^q \lambda_{st}^{pr} + \gamma_s^r \lambda_{tu}^{pr} - \gamma_t^r \lambda_{su}^{pr} + \gamma_u^r \lambda_{st}^{pr} \\ & +\gamma_s^p \gamma_t^q \gamma_u^r - \gamma_s^p \gamma_t^r \gamma_u^q + \gamma_s^q \gamma_t^r \gamma_u^p - \gamma_s^q \gamma_t^p \gamma_u^r \\ & +\gamma_s^r \gamma_t^p \gamma_u^q - \gamma_s^r \gamma_t^q \gamma_u^p \end{aligned} \qquad (10)$$

For the three-particle density matrix, by dropping the three-particle cumulant λ_{stu}^{pqr}, and substituting the expressions (8) and (9) in (10), we obtain an approximate decomposition in terms of one- and two-particle density matrices only

$$\begin{aligned} \gamma_{stu}^{pqr} \Rightarrow {} & \gamma_s^p \gamma_{tu}^{qr} - \gamma_t^p \gamma_{su}^{qr} + \gamma_u^p \gamma_{st}^{qr} \\ & -\gamma_s^q \gamma_{tu}^{pr} + \gamma_t^q \gamma_{su}^{pr} - \gamma_u^q \gamma_{st}^{pr} + \gamma_s^r \gamma_{tu}^{pr} - \gamma_t^r \gamma_{su}^{pr} + \gamma_u^r \gamma_{st}^{pr} \\ & -2(\gamma_s^p \gamma_t^q \gamma_u^r - \gamma_s^p \gamma_t^r \gamma_u^q + \gamma_s^q \gamma_t^r \gamma_u^p - \gamma_s^q \gamma_t^p \gamma_u^r \\ & +\gamma_s^r \gamma_t^p \gamma_u^q - \gamma_s^r \gamma_t^q \gamma_u^p) \\ = {} & 9(\gamma_s^p \wedge \gamma_{tu}^{qr}) - 12(\gamma_s^p \wedge \gamma_t^q \wedge \gamma_u^r) \end{aligned} \qquad (11)$$

To obtain our operator decomposition, we simply replaced expectation values in the above terms by the corresponding operators, i.e. $\gamma_{st}^{pq} \rightarrow a_{st}^{pq}$ and $\gamma_s^p \rightarrow a_s^p$, yielding eqn. (7). Note that by construction, the expectation value of the operator decomposition reproduces the three-particle density matrix cumulant decomposition (11).

By using this decomposition recursively i.e. by constructing the double commutator by first using the decomposed single commutator $[H, A]_{1,2}$ as in eqn. (6), the full effective Hamiltonian $\bar{H}_{1,2}$ at the L-CTSD level *contains only one and two-body operators*. Evaluation of the energy then only requires the one- and two-particle density matrices of the reference function. As discussed in our initial work, this fulfils one of the criteria for an efficient multireference theory, namely, we do not need to

explicitly manipulate the complicated reference function. From a different perspective, the canonical tranformations can also be viewed as providing a parametrisation of a two-particle density matrix theory. Recently, such connections have been explored from a different direction by Mazziotti [32, 33] and while interesting, we shall not dwell further on these matters here.

We call the above formulation a linearised theory, because the operator decomposition is applied at the first commutator. Then, at the L-CTSD level the energies and amplitudes are evaluated via

$$E = \langle \Psi_0 | \bar{H}_{1,2} | \Psi_0 \rangle \qquad (12)$$
$$0 = \langle \Psi_0 | [\bar{H}_{1,2}, a_i^a - a_a^i]_{1,2} | \Psi_0 \rangle \qquad (13)$$
$$0 = \langle \Psi_0 | [\bar{H}_{1,2}, a_{ij}^{ab} - a_{ab}^{ij}]_{1,2} | \Psi_0 \rangle \qquad (14)$$
$$0 = \langle \Psi_0 | [\bar{H}_{1,2}, a_{ij}^{ak} - a_{ak}^{ij}]_{1,2} | \Psi_0 \rangle \qquad (15)$$

The resulting computational cost of the theory is $O(a^2 e^4)$, and is thus comparable to that of a *single-reference* coupled cluster calculation.

B. Accuracy of the operator decomposition

As presented above, the accuracy of the Canonical Transformation theory rests on the accuracy of operator decomposition, given at the L-CTSD level by eqn. (7). However, although our operator decomposition was chosen so that its expectation value would reproduce the density matrix cumulant decomposition, *this choice is not unique.* For example, we could add to the r.h.s. of eqn. (7) any term with vanishing expectation value with Ψ_0 and still preserve the correspondence with the density matrix cumulant decomposition (11). This simply reflects the fact that a decomposition for expectation values (i.e. the cumulant decomposition) does not contain sufficient information to specify a corresponding operator decomposition.

In our earlier work, we examined the accuracy of the operator decomposition through a perturbative analysis of CT theory starting from a single determinantal wavefunction Ψ_D and using a single-reference single-doubles excitation operator $A = A_i^a(a_i^a - a_a^i) + A_{ij}^{ab}(a_{ij}^{ab} - a_{ab}^{ij})$. This analysis showed that the L-CTSD theory was accurate through third-order in the fluctuation potential $W = H - F$ where F is the Fock operator i.e.

$$\begin{aligned} & \langle \Psi_D | \bar{H} | \Psi_D \rangle \\ = {} & \langle \Psi_D | \bar{H}_{1,2} | \Psi_D \rangle + O(W^4) \\ = {} & \langle \Psi_D | H + [H, A]_{1,2} + [[H, A]_{1,2}, A]_{1,2} | \Psi_D \rangle + O(W^4) \end{aligned} \qquad (16)$$

However, consider what happens if we use the more general *multireference* form of A in eqn. (2) that includes semi-internal excitations such as $A_{ij}^{ak}(a_{ij}^{ak} - a_{ak}^{ij})$, together with a single reference wavefunction $|\Psi_D\rangle$. Such excitations should not contribute as they destroy the

single reference wavefunction, and thus all expectation values of exact commutators containing only semi-internal excitations, e.g. $\langle\Psi_D|[H, A_{ij}^{ak}(a_{ij}^{ak} - a_{ak}^{ij})]|\Psi_D\rangle$, $\langle\Psi_D|[[H, A_{ij}^{ak}(a_{ij}^{ak} - a_{ak}^{ij})], A_{lm}^{bn}(a_{lm}^{bn} - a_{bn}^{lm})]|\Psi_D\rangle$ must vanish. However, using the cumulant-based operator decomposition (7) we find that although the expectation value of the first commutator $\langle\Psi_D|[H, A_{ij}^{ak}(a_{ij}^{ak} - a_{ak}^{ij})]_{1,2}|\Psi_D\rangle$, correctly vanishes, it does not do so for the second commutator. Non-vanishing terms arise e.g. from

$$\langle\Psi_D|[[H, A_{ij}^{ak}(a_{ij}^{ak} - a_{ak}^{ij})]_{1,2}, A_{lm}^{bn}(a_{lm}^{bn} - a_{bn}^{lm})]|\Psi_D\rangle \quad (17)$$

Writing H and the two A operators as $g^\dagger g^\dagger gg$, $o^\dagger o^\dagger ov$, $v^\dagger o^\dagger oo$ respectively, using g, o, v to denote general, occupied, and virtual indices respectively, we can see a non-zero contribution arising from

$$\langle\Psi_D|(g^\dagger g^\dagger g\,g)\ (o^\dagger o^\dagger ov)\ (v^\dagger o^\dagger oo)|\Psi_D\rangle \neq 0 \quad (18)$$

where the underbracket denotes contraction and the overbracket denotes a replacement by a density matrix in the operator decomposition.

In a multireference situation, we use the *same* extended excitation operator A (with semi-internal excitations) through the entire potential energy surface, even when the underlying reference wavefunction is largely of a single reference nature, as is sometimes the case near the equilibrium geometry. Thus the above deficiency of the cumulant operator decomposition for single reference wavefunctions motivates us to examine other possible decompositions, as we describe now.

III. EXTENDED NORMAL ORDERING

A. Normal ordering for a Multireference wavefunction

Normal ordering provides a standard way to decompose an operator into a sum of zero-, one-, two- and higher body contributions that are ordered with respect to a given vacuum. In many-body theory it is common to use normal ordering not with respect to the physical vacuum, but rather with respect to a single determinant state or Fermi vacuum. With respect to the Fermi vacuum, normal ordering of the operators $a_s^p, a_{rs}^{pq}, a_{stu}^{pqr}$ yields

$$\tilde{a}_s^p = a_s^p - \delta_s^p n_s \quad (19)$$
$$\tilde{a}_{st}^{pq} = a_{st}^{pq} - \delta_s^p n_s a_t^q - \delta_t^q n_t a_s^p$$
$$+ \delta_t^p n_t a_s^q + \delta_s^q n_s a_t^p + \delta_{st}^{pq} n_p n_q \quad (20)$$
$$\tilde{a}_{stu}^{pqr} = a_{stu}^{pqr} - \delta_s^p n_p a_{tu}^{qr} + \delta_s^q n_q a_{ru}^{pt} + \delta_s^r n_r a_{tu}^{qp}$$
$$+ \delta_t^p n_p a_{su}^{qr} - \delta_t^q n_q a_{su}^{pr} + \delta_t^r n_r a_{su}^{pq} + \delta_u^p n_p a_{ts}^{qr}$$
$$+ \delta q_u n_q a_{st}^{pr} - \delta_u^r n_r a_{st}^{pq} + n_p n_q \delta_{st}^{pq} a_u^r + n_p n_r \delta_{su}^{pr} a_t^q$$
$$+ n_q n_r \delta_{tu}^{qr} a_s^p - n_p n_q \delta_{su}^{pq} a_t^r - n_p n_q \delta_{ut}^{pq} a_s^r - n_p n_r \delta_{st}^{pr} a_u^q$$
$$- n_p n_r \delta_{tu}^{pr} a_s^q - n_q n_r \delta_{ts}^{qr} a_u^p - n_q n_r \delta_{su}^{qr} a_t^p - n_p n_q n_r \delta_{stu}^{pqr} \quad (21)$$

where the tilde represents operators normal-ordered w.r.t. the Fermi vacuum (quasi-particle operators), n_p is the occupation number (0 or 1) of the p-th orbital, and $\delta_{rs}^{pq} = \delta_r^p \delta_s^q - \delta_s^p \delta_r^q$, $\delta_{stu}^{pqr} = \delta_s^p \delta_u^q \delta_u^t + \delta_t^p \delta_u^q \delta_s^r + \delta_u^p \delta_s^q \delta_t^r - \delta_t^p \delta_s^q \delta_u^r - \delta_u^p \delta_t^q \delta_s^r - \delta_s^p \delta_u^q \delta_t^r$. Note that all normal-ordered operators (other than the "zero-body" constant term) yield a vanishing expectation value with the Fermi vacuum, e.g. $\langle\tilde{a}_s^p\rangle = 0$. If we are interested in a state which is well approximated by the Fermi vacuum, the higher-particle rank quasi-particle operators such as $\tilde{a}_{stu}^{pqr}$ are less relevant to its properties than the lower-rank ones, since they represent multiple simultaneous excitations away from the state. Thus the Fermi-vacuum normal ordering presents a natural way to approximate high-particle rank operators in terms of simpler lower-body terms by simply neglecting the high particle-rank quasi-particle operators that appear in the normal ordered form. For example, to approximate a_{stu}^{pqr} in terms of one- and two-body operators alone, we would neglect $\tilde{a}_{stu}^{pqr}$ in eqn. (21).

In the Canonical Transformation theory, however, we are often interested in reference states which cannot be represented well by any Fermi vacuum. Recently, Mukherjee and Kutzelnigg proposed an elegant generalisation of normal-ordering w.r.t. such multireference states [12, 13, 14]. By examining the form of the above normal-ordering equations when rotated into an arbitary one-particle basis, they arrived at the generalised relations

$$a_s^p = \tilde{a}_s^p + \gamma_s^p \quad (22)$$
$$a_{st}^{pq} = \tilde{a}_{st}^{pq} + \gamma_s^p \tilde{a}_t^q + \gamma_t^q \tilde{a}_s^p - \gamma_t^p \tilde{a}_s^q - \gamma_s^q \tilde{a}_t^p + \gamma_{st}^{pq}$$
$$= \tilde{a}_{st}^{pq} + 4(\gamma_s^p \wedge \tilde{a}_t^q) + \gamma_{st}^{pq} \quad (23)$$
$$a_{stu}^{pqr} = \tilde{a}_{stu}^{pqr} + \gamma_s^p \tilde{a}_{tu}^{qr} - \gamma_s^q \tilde{a}_{tu}^{pr} - \gamma_s^r \tilde{a}_{tu}^{qp} - \gamma_t^p \tilde{a}_{su}^{qr} + \gamma_t^q \tilde{a}_{su}^{pr}$$
$$- \gamma_t^r \tilde{a}_{su}^{qr} - \gamma_u^p \tilde{a}_{ts}^{qr} - \gamma_u^q \tilde{a}_{st}^{pr} + \gamma_u^r \tilde{a}_{st}^{pq} + \gamma_{st}^{pq} \tilde{a}_u^r + \gamma_{su}^{pq} \tilde{a}_t^q$$
$$+ \gamma_{tu}^{qr} \tilde{a}_s^p - \gamma_{su}^{pq} \tilde{a}_t^r - \gamma_{ut}^{pq} \tilde{a}_s^r - \gamma_{st}^{pr} \tilde{a}_u^q - \gamma_{tu}^{pr} \tilde{a}_s^q - \gamma_{ts}^{qr} \tilde{a}_u^p$$
$$- \gamma_{su}^{qr} \tilde{a}_t^p + \gamma_{stu}^{pqr}$$
$$= \tilde{a}_{stu}^{pqr} + 9(\gamma_s^p \wedge \tilde{a}_{tu}^{qr}) + 9(\gamma_{st}^{pq} \wedge \tilde{a}_u^r) + \gamma_{stu}^{pqr} \quad (24)$$

Let us examine the physical meaning of the above expressions, taking eqn. (23) as an example. Here, we see that the original two body operator a_{st}^{pq} is written in terms of an average over the reference state (the zero-body operator γ_{st}^{pq}), a product of a one-body average with a one-body quasi-particle operator (the terms like $\gamma_s^p \tilde{a}_t^q$), and a two-body quasi-particle operator $\tilde{a}_{st}^{pq}$. The quasi-particle operators describe fluctuations about the reference, because just as in the usual form of normal ordering, their expectation values with the reference vanish e.g. $\langle\tilde{a}_s^p\rangle = 0, \langle\tilde{a}_{st}^{pq}\rangle = 0$.

B. Application to Canonical Transformation Theory

The extended normal ordering provides a systematic operator decomposition which is well suited to Canonical Transformation theory. At the linearised CTSD level, we

wish to decompose the three-body operators, arising from the commutator $[H, A]$, into lower-body terms. We can do so by neglecting the effects of the simultaneous three-body fluctuations described by the operator $\tilde{a}_{stu}^{pqr}$. For consistency, we should also remove the fully connected three-body cumulant λ_{stu}^{pqr}. First let us rewrite a_{stu}^{pqr} in terms of a_s^p, a_{st}^{pq} be rearranging eqn. (24), and substituting in the cumulant decomposition of γ_{stu}^{pqr} (10), we find

$$
\begin{aligned}
a_{stu}^{pqr} = {}& \tilde{a}_{stu}^{pqr} - \gamma_s^p[a_{tu}^{qr} - \gamma_t^q(a_u^r - \gamma_u^r) + \cdots \\
& - \gamma_{tu}^{qr}] + \cdots - \gamma_{st}^{pq}(a_u^r - \gamma_u^r + \cdots \\
& + \lambda_{stu}^{pqr} + \gamma_s^p\lambda_{tu}^{qr} + \cdots \gamma_s^p\gamma_r^q\gamma_u^t + \cdots \\
= {}& \tilde{a}_{stu}^{pqr} + 9(\gamma_s^p \wedge a_{tu}^{qr}) - 36(\gamma_s^p \wedge \gamma_t^q \wedge a_u^r) + 9(\gamma_{st}^{pq} \wedge a_u^r) \\
& +24(\gamma_s^p \wedge \gamma_t^q \wedge \gamma_u^r) - 9(\gamma_s^p \wedge \gamma_{tu}^{qr}) + \lambda_{stu}^{pqr}
\end{aligned} \tag{25}
$$

Now dropping $\tilde{a}_{stu}^{pqr}$ and λ_{stu}^{pqr} we obtain the extended normal-ordered decomposition, which we name the MK decomposition after Mukherjee and Kutzelnigg,

$$
\begin{aligned}
a_{stu}^{pqr} \Rightarrow {}& 9(\gamma_s^p \wedge a_{tu}^{qr}) - 36(\gamma_s^p \wedge \gamma_t^q \wedge a_u^r) + 9(\gamma_{st}^{pq} \wedge a_u^r) \\
& +24(\gamma_s^p \wedge \gamma_t^q \wedge \gamma_u^r) - 9(\gamma_{st}^{pq} \wedge \gamma_u^r)
\end{aligned} \tag{26}
$$

Comparing the MK decomposition to our earlier cumulant-type decomposition (7) we see that they yield the same expectation value with the reference function Ψ_0 and thus differ only by terms whose expectation values vanish. In addition to some different factors, the MK decomposition include additional operators: a constant term, and the term $\gamma_{st}^{pq} \wedge a_u^r$. Computationally, both these terms are easily implemented without affecting the scaling of the original L-CTSD algorithm.

To better understand the differences between the MK and cumulant-type (CU) decompositions, it is instructive to compare the two for a simpler example, namely, the decomposition of the two-particle operator a_{st}^{pq}. These are

$$
\begin{aligned}
a_{st}^{pq} \Rightarrow {}& 2(\gamma_s^p \wedge a_t^q) \\
= {}& \frac{1}{2}(\gamma_s^p a_t^q + \gamma_t^q a_s^p - \gamma_t^p a_s^q - \gamma_s^q a_t^p) \quad \text{CU}
\end{aligned} \tag{27}
$$

$$
\begin{aligned}
a_{st}^{pq} \Rightarrow {}& \gamma_s^p(a_t^q - \gamma_t^q) + \gamma_t^q(a_s^p - \gamma_s^p) \\
& - \gamma_t^p(a_s^q - \gamma_s^q) - \gamma_s^q(a_t^p - \gamma_t^p) + \gamma_s^p\gamma_t^q - \gamma_t^p\gamma_s^q \quad \text{MK}
\end{aligned} \tag{28}
$$

Here we see that the MK decomposition is expressed in terms of *fluctuations* e.g. $a_s^q - \gamma_s^q$ in the presence of the field γ_t^p, while the cumulant decomposition involves the bare operators a_t^q directly. The neglected term $\tilde{a}_{st}^{pq}$ in the MK decomposition has the conceptual meaning of a simultaneous two-particle fluctuation operator, and we consider this to be conceptually appealing.

Returning to the earlier example that motivated our examination of alternative operator decompositions, let us now look at the normal-product decomposition of commutators involving semi-internal excitation operators, as in eqn. (17). Starting from a single determinantal reference, the extended normal ordering reduces to the usual

TABLE I: Total energies of FCI and differences of various methods from FCI for the simultaneous bond breaking of H_2O molecule with CAS($6e$, $5o$) and cc-pVDZ basis sets. The units are E_{h}. The bond angle is fixed at $<\mathrm{HOH} = 109.57°$. R_e = 0.9929 Å. $\tau_s = 10^{-2}$ and $\tau_d = 10^{-2}$ (described in Sec. VII B) were used in the L-CT calculations. See Ref. [4] for the previous L-CT results.

	$1R_e$	$2R_e$	$3R_e$	$4R_e$
FCI	-76.23885	-75.94558	-75.91003	-75.90872
RHF	0.21718	0.37002	0.57365	0.67159
CASSCF	0.16299	0.13196	0.12302	0.12259
CASPT2	0.01330	0.00843	0.00848	0.00852
CASPT3	0.00377	0.00383	0.00174	0.00158
MR-CI	0.00556	0.00378	0.00296	0.00290
MR-CI+Q	-0.00056	-0.00053	-0.00066	-0.00068
MR-ACPF	0.00093	0.00054	0.00020	0.00017
MR-AQCC	0.00231	0.00150	0.00102	0.00098
CCSD	0.00384	0.02248	0.00967	0.00200
CCSDT	0.00051	-0.00238	-0.04106	-0.04973
L-CTSD(CU)	0.00029	-0.00097	-0.00171	-0.00172
L-CTSD(MK)	-0.00077	-0.00128	-0.00192	-0.00192
previous L-CTD(CU)	0.00219	-0.00056	0.00297	0.00251
previous L-CTSD(CU)	0.00061	-0.00358	0.00301	0.00287

normal ordering with respect to a Fermi vacuum described by eqns (19)-(21). Then, the operator decomposition corresponds to dropping the three-particle normal-ordered operators $\tilde{a}_{stu}^{pqr}$ in eqn. (21). By construction, the remaining normal-ordered operators e.g. $\tilde{a}_{rs}^{pq}$ all have vanishing expectation value with the Fermi vacuum, and consequently using the MK decomposition, the expectation values of all commutators of the form of eqn. (17) with single determinant references *vanish as they should*, in contrast to the cumulant-type decomposition.

Thus we see that the extended normal-ordered MK decomposition offers some conceptual and formal advantages over our earlier cumulant-type CU decomposition. Encouraged by these aspects, we have implemented this decomposition and we now proceed to the numerical results.

IV. CALCULATIONS

A. Water and nitrogen potential energy curves

We performed prototype multireference CT calculations for the simultaneous bond breaking curve of the water molecule and the bond breaking curve of the nitrogen molecule. We chose these molecules to allow a direct comparison with the results in our previous paper with the CU decomposition. [4]. Here we have used a wider range of basis sets, including the cc-pVDZ and cc-pVTZ basis sets for water and 6-31G, cc-pVDZ, and cc-pVTZ basis sets for nitrogen [34, 35].

TABLE II: Total energies of MR-CI+Q and differences of various methods from MR-CI+Q for the simultaneous bond breaking of H_2O molecule with CAS($6e, 5o$) and cc-pVTZ basis sets. The units are E_h. The bond angle is fixed at <HOH = 109.57°. R_e = 0.9929 Å. $\tau_s = 10^{-1}$ and $\tau_d = 10^{-2}$ (described in Sec. VII B) were used in the L-CT calculations.

	$1R_e$	$2R_e$	$3R_e$	$4R_e$
MR-CI+Q	-76.32847	-76.01591	-75.97484	-75.97345
RHF	0.27679	0.41697	0.60895	0.70500
CASSCF	0.22228	0.18279	0.16880	0.16815
CASPT2	0.01545	0.00915	0.00904	0.00911
CASPT3	0.00574	0.00646	0.00307	0.00286
MR-CI	0.01005	0.00761	0.00611	0.00603
MR-ACPF	0.00232	0.00176	0.00139	0.00137
MR-AQCC	0.00467	0.00353	0.00280	0.00277
CCSD	0.00742	0.02995	0.02724	0.01999
CCSDT	-0.00055	-0.00147	-0.03965	-0.04866
L-CTSD(CU)	0.00214	0.00058	-0.00081	-0.00084
L-CTSD(MK)	0.00186	-0.00004	-0.00102	-0.00103

TABLE III: Total energies of FCI and differences of various methods from FCI for the bond breaking of N_2 molecule with CAS($6e, 6o$) and 6-31G basis sets. The Units are E_h. $\tau_s = 10^{-1}$ and $\tau_d = 10^{-2}$ (described in Sec. VII B) were used in the L-CT calculations. See Ref. [4] for the previous L-CT results.

	1Å	2Å	3Å
FCI	-109.04667	-108.85968	-108.83905
RHF	0.21143	0.55008	0.85649
CASSCF	0.08551	0.08623	0.07472
CASPT2	0.01372	0.00834	0.00830
CASPT3	0.00558	0.00769	0.00409
MR-CI	0.00268	0.00303	0.00210
MR-CI+Q	-0.00012	-0.00014	-0.00016
MR-ACPF	0.00092	0.00071	0.00027
MR-AQCC	0.00133	0.00125	0.00069
CCSD	0.00685	-0.00731	
CCSDT	0.00122	-0.05220	
L-CTSD(CU)	0.00142	-0.00165	-0.00173
L-CTSD(MK)	0.00082	-0.00187	-0.00250
previous L-CTD(CU)	0.00510	0.00447	
previous L-CTSD(CU)	0.00646	0.00112	

For assessment, we carried out calculations with state-of-the-art internally contracted multireference methods — second- and third-order perturbation theory (CASPT2 and CASPT3) [36, 37, 38, 39], configuration interaction (MR-CI) [40, 41, 42], the *a posteriori* size-extensivity cor-

rected configuration interaction due to Davidson (MR-CI+Q) [43, 44], averaged coupled pair functional (MR-
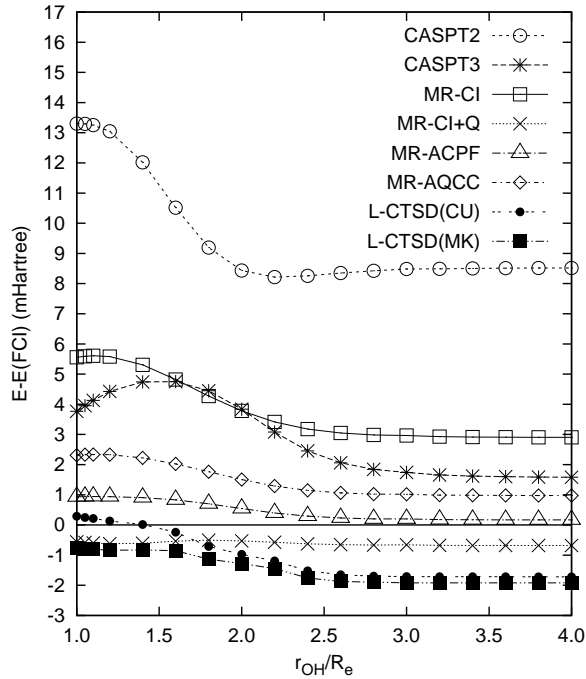

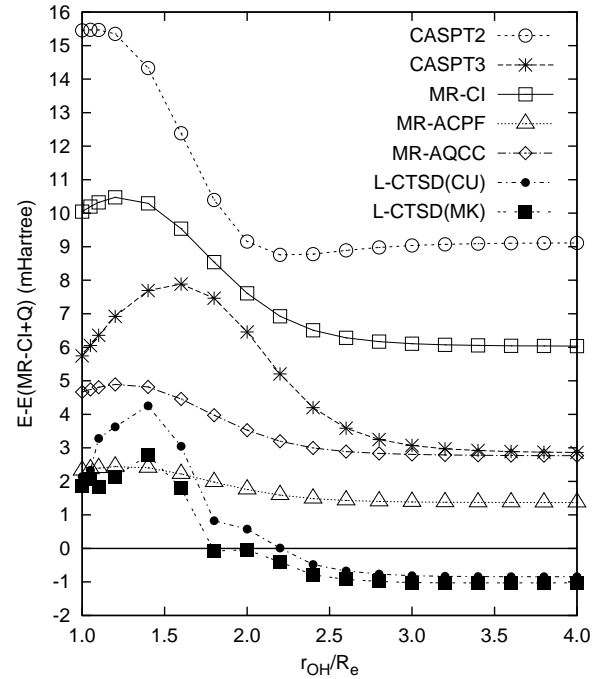FIG. 1: Energy differences E-E(FCI) for the simultaneous bond breaking of H_2O molecule with CAS($6e, 5o$) and cc-pVDZ basis sets.

FIG. 2: Energy differences E-E(MR-CI+Q) for the simultaneous bond breaking of H_2O molecule with CAS($6e, 5o$) and cc-pVTZ basis sets.

TABLE IV: Total energies of MR-CI+Q and differences of various methods from MR-CI+Q for the bond breaking of N_2 molecule with CAS$(6e, 6o)$ and cc-pVDZ basis sets. The units are E_h. $\tau_s = 10^{-1}$ and $\tau_d = 10^{-2}$ (described in Sec. VII B) were used in the L-CT calculations.

	1Å	2Å	3Å
MR-CI+Q	-109.22891	-108.98376	-108.96035
RHF	0.29907	0.65317	0.96627
CASSCF	0.18453	0.19413	0.18316
CASPT2	0.02243	0.01558	0.01616
CASPT3	0.00700	0.00781	0.00375
MR-CI	0.00926	0.01161	0.01011
MR-ACPF	0.00262	0.00245	0.00173
MR-AQCC	0.00419	0.00465	0.00374
CCSD	0.01112	0.07424	
CCSDT	0.00177	-0.04382	
L-CTSD(CU)	0.00118	0.00024	-0.00045
L-CTSD(MK)	0.00117	0.00162	0.00026

TABLE V: Total energies of MR-CI+Q and differences of various methods from MR-CI+Q for the bond breaking of N_2 molecule with CAS$(6e, 6o)$ and cc-pVTZ basis sets. The units are E_h. $\tau_s = 10^{-1}$ and $\tau_d = 10^{-2}$ (described in Sec. VII B) were used in the L-CT calculations.

	1Å	2Å	3Å
MR-CI+Q	-109.33774	-109.05871	-109.03045
RHF	0.36972	0.70119	1.00458
CASSCF	0.25475	0.25035	0.23571
MR-CI	0.01452	0.01725	0.01516
MR-ACPF	0.00363	0.00324	0.00234
MR-AQCC	0.00625	0.00669	0.00548
CASPT2	0.02399	0.01094	0.01195
CASPT3	0.00753	0.01077	0.00396
CCSD	0.01532	0.09593	
CCSDT	0.00021	-0.03276	
L-CTSD(CU)	0.00453[a]	-0.00006	-0.00051
L-CTSD(MK)	0.00249	0.00162	0.00035

a) $\tau_s = 5 \times 10^{-1}$ and $\tau_d = 2 \times 10^{-2}$ were used because of convergence problems.

ACPF) [45, 46] and averaged quadratic coupled-cluster theory (MR-AQCC) [47] (both *a priori* size-extensivity modifications of configuration interaction), as well as single-reference coupled cluster calculations at the CCSD and CCSDT level [48, 49]). Full configuration interaction (FCI) energies were also used for comparison where available. The CAS space for the multireference cal-

culations was six active electrons in five active orbitals [denoted $(6e, 5o)$] for the water calculations and $(6e, 6o)$ for the nitrogen calculations. The $1s$ orbitals in O and N atoms were held frozen in all calculations. For the
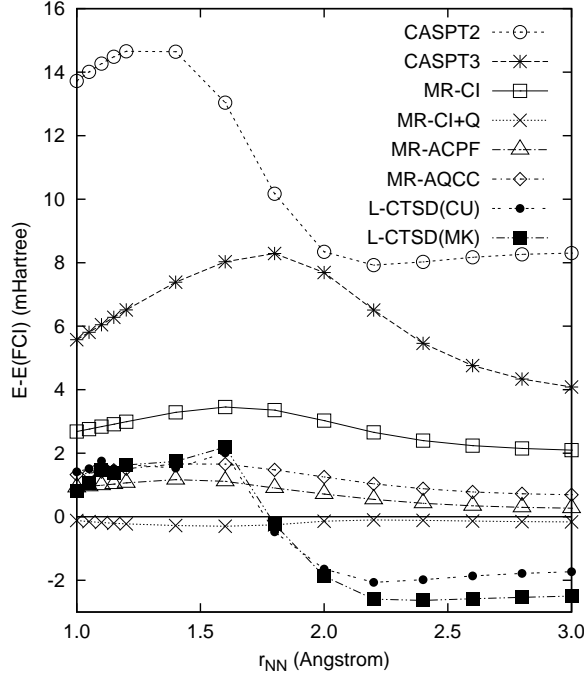

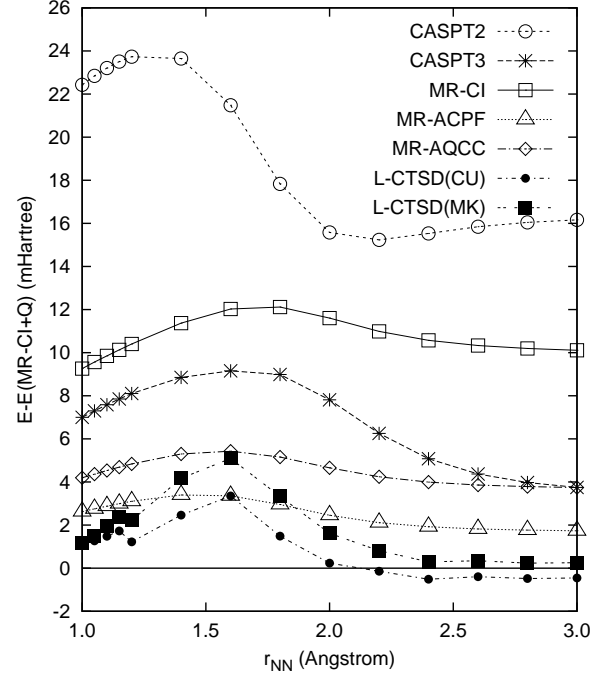FIG. 3: Energy differences E-E(FCI) for the bond breaking of N_2 molecule with CAS$(6e, 6o)$ and 6-31G basis sets.

FIG. 4: Energy differences E-E(MR-CI+Q) for the bond breaking of N_2 molecule with CAS$(6e, 6o)$ and cc-pVDZ basis sets.

L-CTSD calculations, we employed both the cumulant (CU) and normal-ordering (MK) operator decompositions described in section II. The internally-contracted multireference calculations were executed using MOLPRO [56], the CC calculations using TCE [49] in UTCHEM [50], and the CT calculations using our own computer program.

Tables I, II, III, IV, and V present the errors in the total energies of various methods as measured from FCI or (in the larger basis sets) MR-CI+Q at several points across the potential curve. These errors are plotted in Figures 1, 2, 3, 4, and 5.

Comparing all the different methods, in the calculations where FCI energies were available, MR-CI+Q provided the smallest maximum absolute error (MAE) and non-parallelity error (NPE) and for this reason was used as the benchmark method when FCI energies could not be obtained. The general order of accuracy in terms of MAE from most to least accurate was MR-CI+Q $\approx$ MR-ACPF $\approx$ L-CTSD(CU), L-CTSD(MK) $\approx$ MR-AQCC > CASPT3 $\approx$ MR-CI > CASPT2. While the MAE of L-CTSD(CU) and L-CTSD(MK) was comparable to that of MR-ACPF and MR-AQCC, the NPE was larger; in the intermediate region the shapes of the curves somewhat resembled the CASPT3 curve. In the equilibrium region, the L-CTSD energies were similar in accuracy to CCSDT.

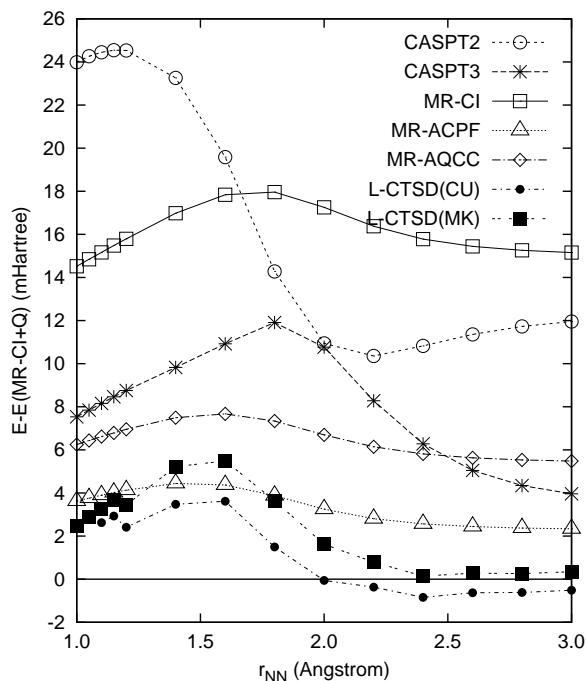The MAE and NPE for the two CT operator decompositions L-CTSD(CU) and L-CTSD(MK) are compared in

TABLE VI: Maximum absolute error (MAE) and non-parallelity error (NPE) of L-CTSD(CU) and L-CTSD(MK). The units are mE_h.

	L-CTSD(CU)		L-CTSD(MK)	
	MAE	NPE	MAE	NPE
H_2O/cc-pVDZ	1.72	2.01	1.92	1.11
H_2O/cc-pVTZ	4.25	5.10	2.79	3.82
N_2/6-31G	2.07	4.08	2.54	4.74
N_2/cc-pVDZ	3.35	3.83	5.09	4.86
N_2/cc-pVTZ	3.62	4.46	5.49	5.35

Table VI. We find that the two operator decompositions performed quite similarly in these systems, although the MAE of L-CTSD(CU) was slightly smaller. For comparison, we have also included the L-CTSD(CU) energies from our calculations in our earlier work [4]. We note that our new L-CTSD(CU) energies are *significantly improved*, particularly in the intermediate dissociation region. This is a result of the new numerical algorithm, described in VII B, which allowed us to significantly reduce the truncation of the operator manifold that we used in our previous work. However, the curves of the new L-CTSD in the figures are not completely smooth due to some remaining operator truncation effects in the numerical solution and removal of this non-smooth behaviour will be addressed in future work.

Table VII shows the spectroscopic constants of N_2 computed by fitting the potential curves. Compared to the available FCI results in the 6-31G basis, MR-CI+Q once again came closest for all spectroscopic parameters (R_e, ω_e, D_e) while the related MR-ACPF and MR-AQCC methods behaved very similarly to MR-CI+Q. Comparing CT against the other methods, different trends were observed for different quantities. For the dissociation energies, we found that MR-CI+Q > MR-ACPF $\approx$ MR-AQCC $\approx$ L-CTSD(CU) > L-CTSD(MK) $\approx$ CCSDT > CASPT3 > CASPT2 > CCSD. For frequencies, in the cc-pVDZ and cc-pVTZ basis L-CTSD was comparable in accuracy to MR-ACPF/MR-AQCC (though with errors in the opposite direction) and better than than those of CCSDT, while the equilibrium bond distances were less accurate than MR-ACPF/MR-AQCC though still comparable to CCSDT. L-CTSD(CU) and L-CTSD(MK) generally performed similarly, although the spectroscopic constants for L-CTSD(CU) with cc-pVTZ could not be obtained because of convergence problems at the fitting geometries. The small non-smoothness in the potential energy curves resulting from the numerical approximations in solving the CT equations may also be a factor in the less systematic errors of the CT methods for R_e and ω_e.

Thus to summarise, the overall performance of L-CTSD(CU) and L-CTSD(MK) for these potential energy curves was competitive with the best multirefer-

FIG. 5: Energy differences E-E(MR-CI+Q) for the bond breaking of N_2 molecule with CAS($6e, 6o$) and cc-pVTZ basis sets.

TABLE VII: Spectroscopic constants for N_2 molecule by various methods with 6-31G, cc-pVDZ, and cc-pVTZ basis sets. The dissociation energy D_e was obtained with additional atomic calculations for the nitrogen atom.

| | R_e | ω_e | D_e |
	Å	cm^{-1}	kcal/mol
6-31G			
FCI	1.134 86	2208.27	168.45
RHF	-0.045 74	452.94	-103.25
CCSD	-0.006 77	77.53	-6.27
CCSDT	-0.002 06	26.93	-1.38
CASSCF	-0.003 77	29.35	-8.87
CASPT2	-0.000 91	3.71	-3.85
CASPT3	-0.001 01	8.80	-1.62
MR-CI	-0.000 33	3.14	-1.24
MR-CI+Q	0.000 10	-0.15	-0.02
MR-ACPF	-0.000 16	1.68	-0.49
MR-AQCC	-0.000 20	1.99	-0.55
L-CTSD(CU)	0.001 11	-15.35	-0.67
L-CTSD(MK)	0.000 53	-10.34	-1.21
cc-pVDZ			
MR-CI+Q	1.120 36	2321.25	200.59
RHF	-0.043 06	436.76	-88.43
CCSD	-0.007 54	87.11	-8.62
CCSDT	-0.001 87	24.90	-1.79
CASSCF	-0.005 89	43.95	-3.58
CASPT2	-0.001 21	4.48	-4.11
CASPT3	-0.001 07	7.77	-2.40
MR-CI	-0.001 10	8.71	-2.83
MR-ACPF	-0.000 47	3.34	-0.48
MR-AQCC	-0.000 62	4.39	-0.48
L-CTSD(CU)	-0.001 25	-4.77	-0.42
L-CTSD(MK)	-0.002 07	-6.20	-1.13
cc-pVTZ			
MR-CI+Q	1.104 76	2332.40	216.00
RHF	-0.037 59	398.68	-95.61
CCSD	-0.008 05	90.91	-8.30
CCSDT	-0.001 65	22.60	-0.15
CASSCF	-0.001 10	18.63	-12.24
CASPT2	-0.000 45	-4.75	-6.99
CASPT3	-0.001 23	10.06	-2.41
MR-CI	-0.001 24	10.58	-4.22
MR-ACPF	-0.000 43	3.09	-0.37
MR-AQCC	-0.000 63	4.87	-0.43
L-CTSD(MK)	-0.002 49	2.02	-1.68
exptl	1.107 68	2358.57	228.4

TABLE VIII: Size consistency errors (mE_h) of CISD, ACPF, AQCC, CCSD, L-CTSD(CU), and L-CTSD(MK) calculations.

	Be + He	Be + 2He	Be + 3He	Be + 4He
CISD	3.10	6.23	9.46	12.83
ACPF	-0.56	-0.76	-0.86	-0.92
AQCC	1.98	2.38	2.66	2.91
CCSD	0.00	0.00	0.00	0.00
L-CTSD(CU)	0.00	0.00	0.00	0.00
L-CTSD(MK)	0.00	0.00	0.00	0.00
	N_2 + He	N_2 + 2He	N_2 + 3He	N_2 + 4He
CISD	1.96	4.00	6.12	8.31
ACPF	-0.41	-0.71	-0.94	-1.11
AQCC	-0.57	-0.98	-1.28	-1.50
CCSD	0.00	0.00	0.00	0.00
L-CTSD(CU)	0.00	0.00	0.00	0.00
L-CTSD(MK)	0.00	0.00	0.00	0.00

ence methods, such as MR-ACPF and MR-AQCC, particularly for energetic quantities such as the MAE and D_e. The shapes of the curves in the intermediate regions looked somewhat like the CASPT3 curves, though with significantly smaller absolute errors. The spectroscopic constants ω_e, R_e and the non-parallelity error from L-CTSD were slightly less accurate than from MR-ACPF and MR-AQCC and this was in part related to our numerical approximations in solving the CT equations.

B. Size-consistency

As is well recognized, size-consistency is a crucial requirement for any correlation model to obtain chemically accurate results in systems with many correlated electrons. As discussed in our initial work [4], the L-CT theory is naturally size-consistent. One way to see this is to observe that the energy is obtained as the expectation value of an effective Hamiltonian that contains only connected contributions by virtue of its construction via a commutator expansion (6). Here we verify the size consistency property of L-CT theory through explicit numerical calculations on supermolecules. We have chosen to use supermolecules that contain more than one type of molecule since certain approximate size-extensive theories such as the ACPF and AQCC methods (which modify the non-size-consistent CISD method) are rigorously size-consistent only in the special case when the supermolecule is made of n noninteracting *identical* subsystems.

Table VIII gives the size consistency errors of L-CTSD, CISD, CCSD, ACPF and AQCC calculations for the Be + n He and N_2 + n He, respectively. All calculations used the HF wavefunction as the reference and the

TABLE IX: Energy difference of all-electron and frozen-core atomic calculations, i.e. $E(\text{all electron}) - E(\text{frozen core})$, by various methods with 6-31G basis sets.

	Be	Ne	Mg	Ar	Ca
FCI	-0.00081	-0.00078	-0.00276	-0.00195	-0.00322
CISD	-0.00075	-0.00077	-0.00252	-0.00187	-0.00292
CCSD(T)	-0.00080	-0.00078	-0.00277	-0.00196	-0.00322
CCSD	-0.00078	-0.00077	-0.00265	-0.00189	-0.00308
AQCC	-0.00156	-0.00098	-0.00452	-0.00205	-0.00505
ACPF	-0.00335	-0.00090	-0.00503	-0.00199	-0.00535
MP3	-0.00099	-0.00076	-0.00275	-0.00185	-0.00324
MP2	-0.00105	-0.00091	-0.00289	-0.00219	-0.00318
L-CTSD(CU)	0.05377	0.11300	0.03612	0.03801	0.02855
L-CTSD(MK)	0.00004	0.00460	-0.00289	0.00660	-0.00320

molecules/atoms were each separated by a distance of 1000 bohr. Size consistency implies the condition $E(\text{A} + n\text{B}) = E(\text{A}) + nE(\text{B})$. As can be seen, the L-CTSD and CCSD calculations are rigorously size-consistent while those of CISD, ACPF and AQCC steadily increase.

Consider now the ACPF energy functional of the non-interacting system $\text{A} + n\text{B}$, given by

$$F_{\text{A}+n\text{B}}^{\text{ACPF}} = \frac{\langle H_\text{A} \rangle + n \langle H_\text{B} \rangle}{1 + (2/N)\langle \delta_\text{A} | \delta_\text{A} \rangle + (2n/N)\langle \delta_\text{B} | \delta_\text{B} \rangle} \quad (29)$$

where $\langle H_\text{A} \rangle = \langle \Psi_\text{A} | H_\text{A} | \Psi_\text{A} \rangle$, N is the total number of electrons, which is equal to $N_A + nN_B$, and δ denotes the orthogonal correlation component of Ψ, e.g. $\Psi_\text{A} = \Psi_{0\text{A}} + \delta_\text{A}$. If $A = B$ in eqn. (29), we readily confirm that $F_{(1+n)\text{B}}^{\text{ACPF}} = (1+n)F_\text{B}^{\text{ACPF}}$ and the energy is size-consistent. The size consistency error in the functional is obtained as,

$$\epsilon(n) = F_{\text{A}+n\text{B}}^{\text{ACPF}} - F_\text{A}^{\text{ACPF}} - n F_\text{B}^{\text{ACPF}}$$
$$= \frac{R_\text{A} R_\text{B}(N_\text{A}\langle H_\text{B} \rangle + N_\text{B}\langle H_\text{A} \rangle) - R_\text{A}^2 N_\text{B}\langle H_\text{B} \rangle - R_\text{B}^2 N_\text{A}\langle H_\text{A} \rangle}{R_\text{A} R_\text{B}^2 + R_\text{A}^2 R_\text{B}/n}$$
$$(30)$$

where $R_\text{A} = N_\text{A} + 2\langle \delta_\text{A} | \delta_\text{A} \rangle$. The errors of ACPF and AQCC indeed appear to behave as the above function. (Note that $\epsilon(n = \infty)$ does not vanish).

C. Density dependence

Rather than considering the scaling behaviour of the energy as we increase the number of molecules, we can also consider the complementary trend of going to atoms with larger and larger nuclear charge Z (and consequently more and more electrons in the same region of space). In essence, this measures the density dependence of the energy. To study the behaviour of the CT and other methods under this condition, we chose five closed-shell atoms, two rare gas atoms (Ne[10e] and Ar[18e]) and three alkaline earth metals (Be[4e], Mg[12e] and Ca[20e]).

Table IX and figure 6 present the core-correlation energies, defined as the energy difference between all-electron and frozen-core atomic calculations, using 6-31G basis sets. The frozen-core calculations correlate eight and two electrons in the valence orbitals for the rare gas atoms and alkaline earth metals, respectively, and represent 98.3% (Be), 99.3% (Ne), 92.1% (Mg), 95.3% (Ar), and 88.7% (Ca) of the all-electron correlation energies. The energy difference between the all-electron and frozen-core calculations is the core correlation energy from the core-valence and core-external excitations. Since we can regard valence-electron correlation as a size-intensive quantity that is described by a fixed, i.e. O(1), small number of valence electrons at a roughly constant valence electron density [57], the rest of the correlation for the bulk of the electrons, i.e. the core correlation, must contain the main density dependence as we change the number of electrons and nuclear charge Z.

Compared to the exact FCI core correlation energies, it is clear that ACPF, AQCC and L-CTSD(CU) have difficulty reproducing the correct behaviour. In particular large errors are found in the ACPF and AQCC calculations for the alkaline earth metals and in the L-CTSD(CU) calculations of the rare gas atoms. By contrast, the size-inconsistent CISD method as well as the MP2 and MP3 methods are able to capture the correct behaviour of the core correlation. This illustrates the difficulty in finding an ad-hoc size-consistency correction, as employed in ACPF and AQCC, that works under all conditions. Most interestingly, the new operator decomposition in L-CTSD(MK) behaves much better than L-CTSD(CU) and reproduces the correct behaviour.

D. FeO binding curve

As a realistic example of a difficult multireference problem, we calculated the potential curve for the ground $1^5\Delta$ state of the FeO molecule. ANO basis sets [51, 52] of DZP quality were used, $[21s15p10d6f]/(5s4p3d1f)$ and $[14s9p4d]/(3s2p1d)$ for the Fe and O basis, respectively. To facilitate the setup for the multireference calculations,

TABLE X: Total energies of MR-CI+Q (E_h) and differences (mE_h) of various methods from MR-CI+Q for the ground $1^5\Delta$ state of FeO molecule.

	1.50Å	1.57Å	1.65Å	1.72Å	2.00Å
MRCI+Q	-1337.65843	-1337.67007	-1337.67302	-1337.66923	-1337.62980
CASSCF	299.22	294.87	290.00	284.82	265.74
CASPT2	-8.20	-7.14	-5.73	-4.12	0.57
CASPT3	41.79	41.78	40.57	38.46	28.73
MRCI	21.78	21.41	20.93	20.37	17.92
MRACPF	0.51	0.40	0.32	0.29	0.45
MRAQCC	4.61	4.46	4.30	4.16	3.79
L-CTSD(CU)[a]	c	c	9.17	9.43	7.67
L-CTSD(CU)[b]	c	c	6.85	6.85	3.51
L-CTSD(MK)[a]	3.09	2.73	3.00	3.85	3.52
L-CTSD(MK)[b]	0.83	1.21	1.66	2.25	-0.16

a) $\tau_s = 3.0 \times 10^{-1}$ and $\tau_d = 5.0 \times 10^{-2}$.
b) $\tau_s = 1.5 \times 10^{-1}$ and $\tau_d = 5.0 \times 10^{-2}$.
c) Not converged.
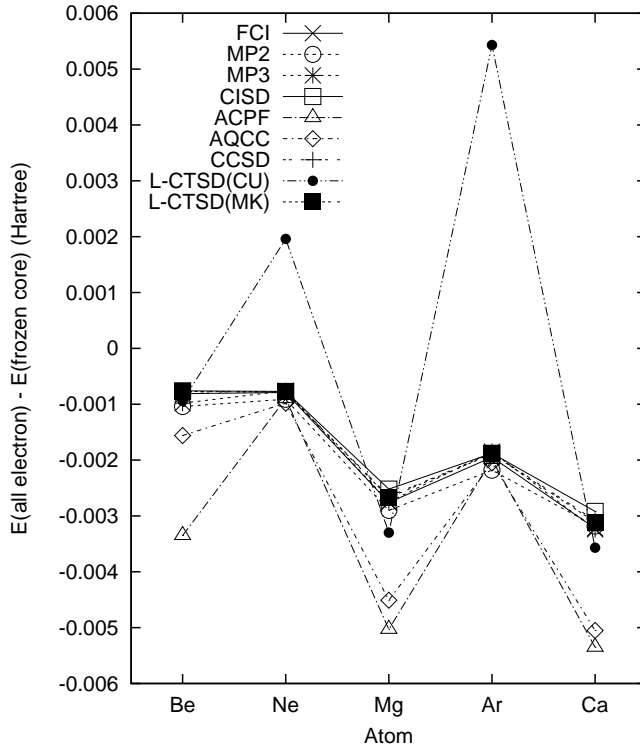
FIG. 6: Density scaling: Energy difference E(all electron) $-$ E(frozen core) for atomic calculations shown in Tables IX.

were held frozen for the CASSCF and subsequent dynamic correlation calculations. We verified that the errors made by this orbital restriction were almost constant within 1 mE_h and thus would not affect the shapes of the potential curves. The orbital $(7\sigma)^2$ was treated as an external core orbital, which was optimized by CASSCF and then correlated. The remaining 12 electrons were fully correlated with 12 active orbitals

$$(8\sigma)^2(9\sigma)^1(10\sigma)^0(11\sigma)^0(3\pi)^4(4\pi)^2(5\pi)^0(1\delta)^3 \quad (32)$$

(the occupations are based on the ROHF configuration of the $^5\Delta$ state) for CAS denoted as $(12e, 12o)$. This CAS is derived from Fe $3d$ and $4s$ orbitals, oxygen $2p$ orbitals, and the third bonding and antibonding π orbitals, which

TABLE XI: Spectroscopic constants for the ground $1^5\Delta$ state of FeO molecule.

	R_e(Å)	ω_e(cm^{-1})
CASSCF	1.703	691.1
CASPT2	1.620	913.8
CASPT3	1.657	755.2
MR-CI	1.641	844.4
MR-CI+Q	1.635	863.2
MR-ACPF	1.636	863.5
MR-AQCC	1.637	858.7
L-CTSD(MK)[a]	1.631	914.0
L-CTSD(MK)[b]	1.630	911.1
exptl.	1.616	880

a) $\tau_s = 3.0 \times 10^{-1}$ and $\tau_d = 5.0 \times 10^{-2}$.
b) $\tau_s = 1.5 \times 10^{-1}$ and $\tau_d = 5.0 \times 10^{-2}$.

the initial orbitals were obtained from closed-shell RHF calculations for the $1^1\Sigma$ state. The ten lowest lying orbitals for 20 electrons

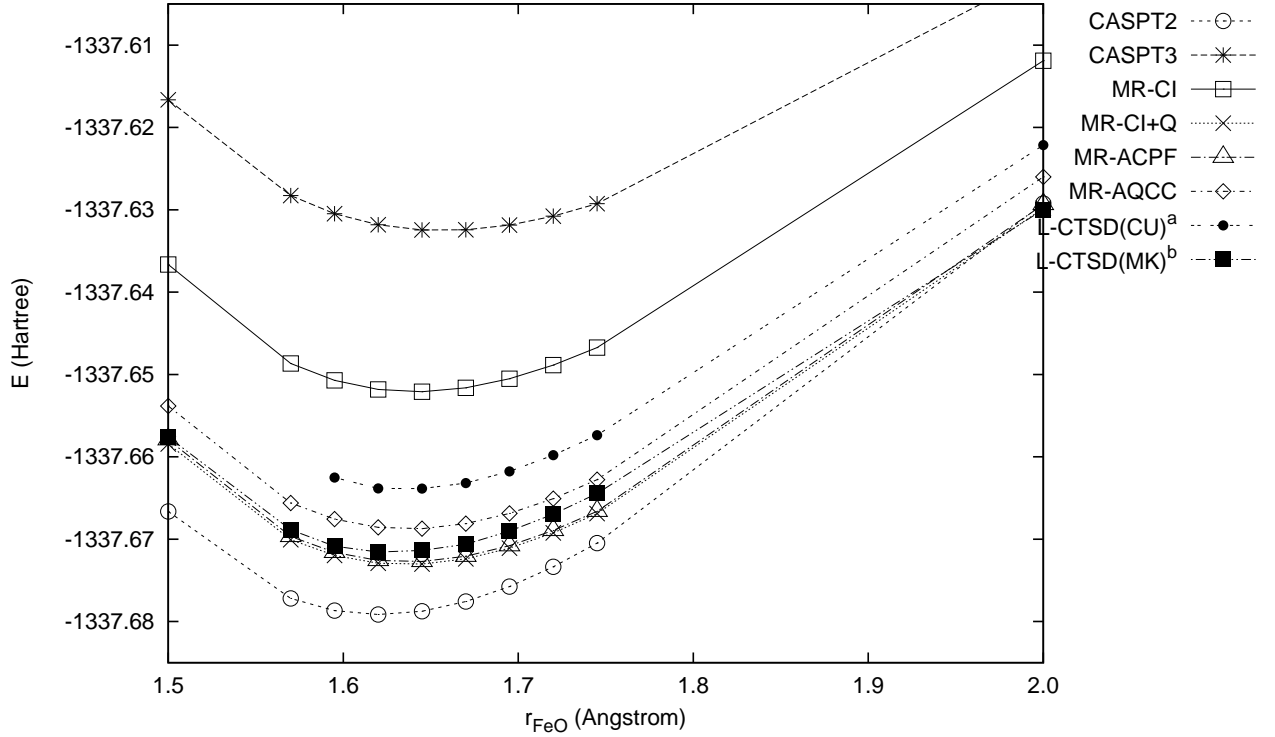$$(1\sigma)^2(2\sigma)^2(3\sigma)^2(4\sigma)^2(5\sigma)^2(6\sigma)^2(1\pi)^4(2\pi)^4 \quad (31)$$

FIG. 7: Potential curve for the ground $1^5\Delta$ state of FeO molecule. a) $\tau_s = 3.0 \times 10^{-1}$ and $\tau_d = 5.0 \times 10^{-2}$. b) $\tau_s = 1.5 \times 10^{-1}$ and $\tau_d = 5.0 \times 10^{-2}$.

are formed from the oxygen $2p_\sigma$ orbital mixing with some Fe $4p_\sigma$ [53, 54].

Figure 7 shows the potential curves of FeO computed by various multireference methods. As exact energies are not available for this system, we report the differences from MR-CI+Q energies in Table X. Clearly, the MR-ACPF, MR-AQCC, and L-CTSD(MK) curves are all very close to each other, while the MR-CI and CASPT2/CASPT3 curves are significantly further away. The MR-ACPF curve follows the MR-CI+Q curve with deviations of less than 0.5 mE_h, while the MR-AQCC curve is also nearly parallel with deviations of 3.8-4.6 mE_h. The L-CTSD(CU) and L-CTSD(MK) curves were shifted relative to each other; the L-CTSD(MK) energies were significantly closer to the MRCI+Q energies, with deviations of less than 2.3 mE_h. CASPT2 seemed to overestimate the correlation energy, while going to the third order CASPT3 over-corrected too much in the opposite direction and strongly underestimated the correlation energy.

Table XI shows the spectroscopic constants measured from the potential curves. While the basis used is probably too small for direct comparison to experiment, we see that in relation to the experimental results, MR-CI and related modifications MR-CI+Q, MR-ACPF and MR-AQCC give frequencies that are too low and bond-lengths that are too long, while L-CTSD(MK) gives frequencies that are too high and slightly improved bond-lengths.

As we have already seen in the difference between the CASPT2 and CASPT3 curves, multireference perturbation theory seemed to break down in this molecule.

E. Timings

It is our intention that the CT theory should be practically applicable to problems of reasonable size, and let us now examine the computational timings for the multireference calculations on the FeO molecule we have just discussed. These are shown in Table XII. All timings were obtained on a single CPU of the Altex system (Itanium 1.5GHz) at the Research Center for Computational Science, Okazaki. As can be seen, the MR-CI based methods were two to three orders of magnitude more expensive than CASPT2. L-CTSD(MK) displayed very satisfactory performance. Even in our protopyte CT implementation, which did not use point-group symmetry, the single-point energy calculation *took less time than even the CASPT2 calculation, while providing a significantly better accuracy competitive with MR-ACPF.*

V. SUMMARY AND CONCLUSIONS

We have been developing the Canonical Transformation theory to describe dynamic correlation in multiref-

erence problems. The theory uses a size-extensive unitary exponential acting on a multireference function. In our initial work, we introduced a central approximation that rendered the manipulation of this ansatz practical, namely a cumulant-based operator decomposition. This choice of decomposition is not unique, however, and in the current work we introduced a new operator decomposition, based on the extended normal ordering of Mukherjee and Kutzelnigg [12, 13, 14], which possesses attractive formal and conceptual features.

We carried out calculations at the Linearised Canononical Transformation Theory Singles and Doubles (L-CTSD) level using both our earlier cumulant-based and current Mukherjee-Kutzelnigg operator decompositions. In studies of the water, nitrogen, and iron-oxide binding curves, we found the accuracy of L-CTSD to be competitive with some of the best existing multireference methods such as the Multireference Averaged Coupled Pair Functional, while the computational cost was two-three orders of magnitude less and comparable to that of Complete-Active-Space Second Order Perturbation Theory. Compared to our earlier work, our results and computational timings were greatly improved, in part due to the use of a new numerical algorithm for converging the Canonical Transformation equations.

VI.   ACKNOWLEDGEMENTS

TABLE XII: Timings for different multireference methods for a single point calculation on the FeO curve. Note that the L-CTSD calculation did not use point-group symmetry, while C_{2v} symmetry was used in all the other calculations. The time for the CASSCF calculation is not included.

	Time/s
CASPT2	5900
CASPT3	17000
MR-CI+Q	158000
MR-ACPF	168000
L-CTSD(MK)[a]	4500

a) The time for constructing density matrices is not included.

VII.   APPENDIX: IMPLEMENTING CANONICAL TRANSFORMATION THEORY

A.   Recapitulation

In our previous implementation of the CT algorithm [4] we solved the residual equations using the following skeletal algorithm

1. Set up the electronic Hamiltonian H and the one- and two-particle density matrices of a reference wavefunction.

2. Compute the transformed Hamiltonian $\bar{H}_{1,2}$ (eqn. (6)).

3. Compute the residuals of CT amplitude equations.

$$R_s^p = \langle [\bar{H}_{1,2}, a_s^p - a_p^s]_{1,2} \rangle \qquad (33)$$

$$R_{st}^{pq} = \langle [\bar{H}_{1,2}, a_{st}^{pq} - a_{pq}^{st}]_{1,2} \rangle \qquad (34)$$

4. Update the amplitudes by adding the preconditioned residuals

$$A_s^p \leftarrow A_s^p - R_s^p / D_s^p \qquad (35)$$

$$A_{st}^{pq} \leftarrow A_{st}^{pq} - R_{st}^{pq} / D_{st}^{pq} \qquad (36)$$

where the factors $1/D_s^p$ and $1/D_{st}^{pq}$ are the diagonal preconditioners.

5. Repeat (2)-(4) until convergence.

In addition, we employed a somewhat complicated division of the optimisation process into different steps involving different classes of excitations in the A operator.

B.   Preconditioning and orthogonalisation

Our primary concern in the current implementation was to improve the convergence of the CT equations. To achieve this, instead of using a diagonal preconditioner as in (35), (36), we updated the amplitudes through an exact Newton step. The simplest way to define the Newton update is through the linear equation

$$D_{s,y}^{p,v} \Delta A_y^v = -R_s^p \qquad (37)$$

$$D_{st,yz}^{pq,vw} \Delta A_{yz}^{vw} = -R_{st}^{pq} \qquad (38)$$

with

$$D_{s,y}^{p,v} = \langle [[\bar{H}_{1,2}, a_y^v - a_v^y]_{1,2}, a_s^p - a_p^s]_{1,2} \rangle \qquad (39)$$

$$D_{st,yz}^{pq,vw} = \langle [[\bar{H}_{1,2}, a_{yz}^{vw} - a_{vw}^{yz}]_{1,2}, a_{st}^{pq} - a_{pq}^{st}]_{1,2} \rangle \qquad (40)$$

We can interpret the D matrices as the derivatives of the residual or Hessians of the energy. However, eqns. (39), (40) are non-optimal as the search directions (i.e. the components of A) within the first-order interacting

space, namely the singly-external, doubly-external, and semi-internal excitations

$$(a_a^i - a_i^a)\Psi_0 \tag{41}$$

$$(a_{ij}^{ab} - a_{ab}^{ij})\Psi_0 \tag{42}$$

$$(a_{ij}^{ak} - a_{ak}^{ij})\Psi_0 \tag{43}$$

generate a non-orthogonal and even linearly-dependent basis. The large spread in eigenvalues of the overlap of the first-order interacting basis (41), (42), (43) can then cause poor convergence of the linear equations (37) and (38).

To remedy this, we first orthogonalise the first-order interacting basis by diagonalising the overlap matrix S made of the one, two, and three-particle density matrices,

$$S_{i,j} = \langle (a_i^a - a_a^i)^\dagger (a_j^a - a_a^j) \rangle$$
$$= \gamma_j^i \tag{44}$$

$$S_{i,jkl} = \langle (a_i^a - a_a^i)^\dagger (a_{jk}^{al} - a_{al}^{jk}) \rangle$$
$$= \gamma_{jk}^{il} \tag{45}$$

$$S_{ijk,lmn} = \langle (a_{ij}^{ak} - a_{ak}^{ij})^\dagger (a_{lm}^{an} - a_{an}^{lm}) \rangle$$
$$= \delta_{kn}\gamma_{lm}^{ij} - \gamma_{lmk}^{ijn} \tag{46}$$

$$S_{ij,kl} = \langle (a_{ij}^{ab} - a_{ab}^{ij})^\dagger (a_{kl}^{ab} - a_{ab}^{kl}) \rangle \quad (a \neq b)$$
$$= \gamma_{kl}^{ij} \tag{47}$$

and change to the orthogonalised excitation operators a_μ^a and a_ν^{ab}

$$a_\mu^a = S_{\mu,i}^{-1/2}(a_i^a - a_a^i) + S_{\mu,ijk}^{-1/2}(a_{ij}^{ak} - a_{ak}^{ij}) \tag{48}$$

$$a_\nu^{ab} = S_{\nu,ij}^{-1/2}(a_{ij}^{ab} - a_{ab}^{ij}) \tag{49}$$

We can then solve the Newton equations (37), (38) in this orthogonalised representation. To do so, the quantities A, R, and D are re-expressed in terms of a_μ^a and a_ν^{ab}

$$A = \tilde{A}_\mu^a a_\mu^a + \tilde{A}_\nu^{ab} a_\nu^{ab} \tag{50}$$

$$\tilde{R}_\mu^a = \langle [\bar{H}_{1,2}, a_\mu^a - a_a^\mu]_{1,2} \rangle \tag{51}$$

$$\tilde{R}_\mu^{ab} = \langle [\bar{H}_{1,2}, a_\mu^{ab} - a_{ab}^\mu]_{1,2} \rangle \tag{52}$$

$$\tilde{D}_{\mu,\nu}^{a,b} = \langle [[\bar{H}_{1,2}, a_b^b - a_b^\nu]_{1,2}, a_\mu^a - a_a^\mu]_{1,2} \rangle \tag{53}$$

$$\tilde{D}_{\mu,\nu}^{ab,cd} = \langle [[\bar{H}_{1,2}, a_\nu^{cd} - a_{cd}^\nu]_{1,2}, a_\mu^{ab} - a_{ab}^\mu]_{1,2} \rangle \tag{54}$$

The numbers of operators a_μ^a and a_ν^{ab} are $O(a^3 e)$ and $O(a^2 e^2)$, respectively. Thus the additional cost of the transformation is $O(a^6 e)$ for the terms involving a_μ^a and $O(a^4 e^2)$ for the terms involving a_ν^{ab}. The diagonalisation of the overlap matrix S for the semi-internal and singly-external (i.e. eqn. (44)-(46)) requires a cost of $O(a^9)$. While the scaling of these steps is relatively high, they are not expected to be a bottleneck for systems where conventional CASSCF calculations can be performed (for example, internally contracted CASPT2 also contains steps

with such cost [36, 37]). However, if we were to use a large active space arising from e.g. a DMRG calculation, a different algorithm should be used.

Let us consider now the condition number of $\tilde{D}$ and the convergence characteristics of the Newton equations in the orthogonalised representation. If D were formed *without* any operator decomposition approximation, then $\tilde{D}$ would represent the true Hessian of the energy with respect to an orthogonal set of directions in the first-order interacting space. The condition number of $\tilde{D}$ would then be governed by the excitation energy between the reference and excited states, which could be expected to be reasonable in most systems. Loosely speaking, we can regard the improved condition number of $\tilde{D}$ as arising from the cancellation of small eigenvalues of D by the large eigenvalues of $S^{-1/2}$. However, such a cancellation is unstable, if we approximate D using the operator decomposition. Therefore to further improve the condition number of $\tilde{D}$ we discarded those operators a_μ^a and a_ν^{ab} which corresponded to small eigenvalues of S. The eigenvalue truncation thresholds are denoted hereafter as τ_s for the singly external and semi-internal and τ_d for the doubly external excitations. This limits the largest linear combination amplitude coefficients (e.g. $S_{\mu,i}^{-1/2}$) appearing in eqns. (48), (49) to $O(\tau_s^{-1/2})$ and $O(\tau_d^{-1/2})$ respectively, preserving numerical stability in the amplitude equations. Typically, we used $\tau_s < 10^{-1}$ and $\tau_d < 10^{-2}$. These cutoffs appear large because of the extreme degeneracy of the first-order interacting space near equilibrium, and because of the incomplete removal of the poorly conditioned components, due to the slight incompatibility (unstable cancellation) between the approximate Hessian and the overlap matrix in this space. Linear dependency is particularly strong near equilibrium because some of the active orbitals which are being excited by A have nearly zero occupancy. However, the contribution of the neglected terms to the energy is small. For N_2 with the cc-pVDZ basis, the size of the effective orthogonalised operator space was 410 ($R_{NN} = 1.0$), 698 ($R_{NN} = 1.6$), and 938 ($R_{NN} = 3.0$) indicating that over 50% of the operator basis was truncated near equilibrium. In the dissociation region of the potential energy curves studied here, truncation did not occur.

In our previous work, we encountered numerical difficulties in using singly external excitation operators in conjunction with doubles, i.e. for L-CTSD. We now see that the reason is the linear dependency between singly external and semi-internal excitations, which appears as non-zero overlap in $S_{i,jkl}$ (eqn. (45)). The orthogonalisation fixes this issue, and thus we have used L-CTSD as the standard L-CT model in this work. This should be naturally superior to L-CTD as it includes orbital relaxation and extra correlation such as three- or higher-particle excitations from the direct product of singles and doubles.

Using the Newton update as described above, we observed efficient convergence in the CT amplitude equa-

TABLE XIII: The total energies (E_h) of L-CTSD(MK) for the bond breaking of the N_2 molecule with CAS($6e, 6o$) and various basis sets using the exact and approximate (cumulant) three-particle density matrices for orthogonalisation.

	$1\mathring{A}$	$2\mathring{A}$	$3\mathring{A}$
6-31G			
exact orthog.	-109.04585	-108.86156	-108.84155
cumulant orthog.	-109.04566	-108.86220	-108.84155
diff (mE_h)	+0.19	-0.64	0.0
cc-pVDZ			
exact orthog.	-109.22774	-108.98214	-108.96009
cumulant orthog.	-109.22752	-108.98305	-108.96009
diff (mE_h)	+0.22	-0.91	0.0
cc-pVTZ			
exact orthog.	-109.33525	-109.05709	-109.03011
cumulant orthog.	not conv.	-109.05824	-109.03011
diff (mE_h)		-1.15	0.0

tions. Typically only 10 Newton steps would be required to converge the amplitudes in multireference calculations. Convergence behavior of the amplitude equations in L-CTSD(CU) and L-CTSD(MK) was generally similar, but there were some cases where we could converge the L-CTSD(MK) but not the L-CTSD(CU) calculations

with the standard truncation thresholds, for example at $R_{NN} = 1\mathring{A}$ for N_2 (cc-pVTZ), as discussed in Sec. IV A.

C. Operator orthogonalisation with cumulant density matrix

Rather than using the exact three-particle density matrix for the orthogonalisation procedure described above, we could also imagine using its cumulant decomposition in terms of the one- and two-particle density matrices, eqn. (10).

Table XIII shows the differences of the total energies computed using the amplitude operators that are orthogonalised with the exact and approximate (cumulant) three-particle density matrices for the N_2 potential energy curves discussed in section IV A. With the truncation threshold $\tau_s = 10^{-1}$ and $\tau_d = 10^{-2}$ and using various basis sets, the energies from both orthogonalisations were generally in good agreement within a deviation of 1.2 mE_h. However, at $R_{NN} = 1.0\mathring{A}$ with the cc-pVTZ basis set, the L-CTSD(MK) calculation with the cumulant based orthogonalisation did not converge.

[1] R. J. Bartlett and J. F. Stanton, Rev. Comput. Chem. **5**, 65 (1994).
[2] T. Helgaker, T. A. Ruden, P. Jørgensen, J. Olsen, and W. Klopper, J. Phys. Org. Chem. **17**, 913 (2004).
[3] T. J. Lee and G. E. Scuseria, in *Quantum Mechanical Electronic Structure Calculations with Chemical Accuracy*, edited by S. R. Langhoff, volume 2, pages 47–108, Kluwer Academic Publishers, Dordrecht, 1995.
[4] T. Yanai and G. K.-L. Chan, J. Chem. Phys. **124**, 194106 (2006).
[5] S. R. White, J. Chem. Phys. **117**, 7472 (2002).
[6] F. Colmenero and C. Valdemoro, Phys. Rev. A **47**, 979 (1993).
[7] F. Colmenero and C. Valdemoro, Int. J. Quantum Chem. **51**, 369 (1994).
[8] H. Nakatsuji and K. Yasuda, Phys. Rev. Lett. **76**, 1039 (1996).
[9] K. Yasuda and H. Nakatsuji, Phys. Rev. A **56**, 2648 (1997).
[10] D. A. Mazziotti, Phys. Rev. A **57**, 4219 (1998).
[11] D. A. Mazziotti, Chem. Phys. Lett. **289**, 419 (1998).
[12] D. Mukherjee, in *Recent Progress in Many-Body Theories*, edited by E. Schachinger, H. Mitter, and H. Sormann, volume 4, page 127, Plenum, New York, 1995.
[13] D. Mukherjee, Chem. Phys. Lett. **274**, 561 (1997).
[14] W. Kutzelnigg and D. Mukherjee, J. Chem. Phys. **107**, 432 (1997).
[15] B. O. Roos, Adv. Chem. Phys. **69**, 399 (1987).
[16] K. Ruedenberg, M. W. Schmidt, M. M. Gilbert, and S. T. Elbert, Chem. Phys. **71**, 41 (1982).
[17] G. K.-L. Chan and M. Head-Gordon, J. Chem. Phys. **116**, 4462 (2002).
[18] J. Hachmann, W. Cardoen, and G. K.-L. Chan, J. Chem. Phys. **125**, 144101 (2006).
[19] J. Paldus and X. Li, Adv. Chem. Phys. **110**, 1 (1999).
[20] K. F. Freed, in *Many-Body Methods in Quantum Chemistry*, edited by U. Kaldor, page 1, Springer, Berlin, 1989.
[21] B. Kirtman, J. Chem. Phys. **75**, 798 (1981).
[22] M. R. Hoffmann and J. Simons, J. Chem. Phys. **88**, 993 (1988).
[23] W. Kutzelnigg, J. Chem. Phys. **77**, 3081 (1982).
[24] W. Kutzelnigg, J. Chem. Phys. **80**, 822 (1984).
[25] J. D. Watts, G. W. Trucks, and R. J. Bartlett, Chem. Phys. Lett. **157**, 359 (1989).
[26] R. J. Bartlett, S. A. Kucharski, and J. Noga, Chem. Phys. Lett. **155**, 133 (1989).
[27] A. G. Taube and R. J. Bartlett, Int. J. Quantum Chem. **106**, 3393 (2006).
[28] S. Pal, M. D. Prasad, and D. Mukherjee, Theor. Chim. Acta **62**, 523 (1983).
[29] S. Pal, Theor. Chim. Acta **66**, 207 (1984).
[30] J. H. van Vleck, Phys. Rev. **33**, 467 (1929).
[31] W. Kutzelnigg and D. Mukherjee, J. Chem. Phys. **110**, 2800 (1999).
[32] D. A. Mazziotti, Phys. Rev. Lett. **97**, 143002 (2006).
[33] D. A. Mazziotti, Phys. Rev. A **75**, 022505 (2007).

[34] W. J. Hehre, R. Ditchfield, and J. A. Pople, J. Chem. Phys. **56**, 2257 (1972).

[35] T. H. Dunning, Jr, J. Chem. Phys. **90**, 1007 (1989).

[36] K. Andersson, P.-Å. Malmqvist, B. O. Roos, A. J. Sadlej, and K. Wolinski, J. Phys. Chem. **94**, 5483 (1990).

[37] K. Andersson, P.-Å. Malmqvist, and B. O. Roos, J. Chem. Phys. **96**, 1218 (1992).

[38] H.-J. Werner, Mol. Phys. **89**, 645 (1996).

[39] P. Celani and H.-J. Werner, J. Chem. Phys. **112**, 5546 (2000).

[40] H.-J. Werner and E. A. Reinsch, J. Chem. Phys. **76**, 3144 (1982).

[41] H.-J. Werner and P. J. Knowles, J. Chem. Phys. **89**, 5803 (1988).

[42] P. J. Knowles and H.-J. Werner, Chem. Phys. Lett. **145**, 514 (1988).

[43] S. R. Langoff and E. R. Davidson, Int. J. Quantum Chem **8**, 61 (1974).

[44] E. R. Davidson and D. W. Silver, Chem. Phys. Lett. **52**, 403 (1977).

[45] R. J. Gdanitz and R. Ahlrichs, Chem. Phys. Lett. **143**, 413 (1988).

[46] H.-J. Werner and P. J. Knowles, Theor. Chim Acta **78**, 175 (1990).

[47] P. G. Szalay and R. J. Bartlett, Chem. Phys. Lett. **214**, 481 (1993).

[48] R. J. Bartlett, in *Modern Electronic Structure Theory*, edited by D. R. Yarkony, Advanced Series in Physical Chemistry, pages 1047–1131, World Scientific, River Edge, NJ, 1995.

[49] S. Hirata, J. Phys. Chem. A **107**, 4940 (2003).

[50] T. Yanai et al., Utchem – a program for ab initio quantum chemistry., in *Lecture Notes in Computer Science*, pages 84–95, Berlin, 2003, Springer-Verlag.

[51] P. O. Widmark, P. Å. Malmqvist, and B. O. Roos, Theor. Chim. Acta **77**, 291 (1990).

[52] R. Pou-Amérigo, M. Merchán, I. Nebot-Gil, P. O. Widmark, and B. O. Roos, Theor. Chim. Acta **92**, 149 (1995).

[53] C. W. Bauschlicher, S. R. Langhoff, and A. Komornicki, Theor. Chim. Acta **77**, 263 (1990).

[54] J. F. Harrison, Chem. Rev. **100**, 679 (2000).

[55] Coupled cluster theory may similarly be viewed as involving two sets of approximations: truncation of the excitation operators, and approximate solution of the Schrödinger equation in a restricted projected space of excitations

[56] MOLPRO, version 2006.1, a package of ab initio programs, H.-J. Werner, P. J. Knowles, R. Lindh, F. R. Manby, M. Schtz, and others

[57] This separation of core and valence densities can be made precise in Thomas-Fermi theory, see e.g. E. H. Lieb, Rev. Mod. Phys. **48**, 553 (1976).